Journal of Photochemistry & Photobiology, B: Biology 164 (2016) 73–82

Contents lists available at ScienceDirect

Journal of Photochemistry & Photobiology, B: Biology

journal homepage: www.elsevier.com/locate/jphotobiol

Purple-bacterial photosynthetic reaction centers and quantum-dot hybrid-assemblies in lecithin liposomes and thin films

Eugeny P. Lukashev [a], Petr P. Knox [a], Vladimir V. Gorokhov [a], Nadezda P. Grishanova [a], Nuranija Kh. Seifullina [a], Maria Krikunova [b], Heiko Lokstein [c], Vladimir Z. Paschenko [a,*]

[a] Biology Faculty, Lomonosov Moscow State University, 119991 Moscow, Russia
[b] Institut für Optik und Atomare Physik, Technische Universität Berlin, Strasse des 17 Juni 135, ER 1-1, D-10623 Berlin, Germany
[c] Charles University, Department of Chemical Physics and Optics, Ke Karlovu 3, 121 16 Prague, Czech Republic

ARTICLE INFO

Article history:
Received 17 June 2016
Accepted 6 September 2016
Available online 12 September 2016

Keywords:
Light-harvesting
Quantum dots
Reaction centers
Pigment–protein complexes
Lecithin liposomes
Fluorescence
Hybrid complexes

ABSTRACT

Quantum dots (QDs) absorb ultraviolet and long-wavelength visible light energy much more efficiently than natural bacterial light-harvesting proteins and can transfer the excitation energy to photosynthetic reaction centers (RCs). Inclusion of RCs combined with QDs as antennae into liposomes opens new opportunities for using such hybrid systems as a basis for artificial energy-transforming devices that potentially can operate with greater efficiency and stability than devices based only on biological components or inorganic components alone.
RCs from *Rhodobacter sphaeroides* and QDs (CdSe/ZnS with hydrophilic covering) were embedded in lecithin liposomes by extrusion of a solution of multilayer lipid vesicles through a polycarbonate membrane or by dialysis of lipids and proteins dispersed with excess detergent. The efficiency of RC and QD interaction within the liposomes was estimated using fluorescence excitation spectra of the photoactive bacteriochlorophyll of the RCs and by measuring the fluorescence decay kinetics of the QDs. The functional activity of the RCs in hybrid complexes was fully maintained, and their stability was even increased. The efficiency of energy transfer between QDs and RCs and conditions of long-term stability of function of such hybrid complexes in film preparations were investigated as well. It was found that dry films containing RCs and QDs, maintained at atmospheric humidity, are capable of maintaining their functional activity for at least some months as judged by measurements of their spectral characteristics, efficiency of energy transfer from QDs to RCs and RC electron transport activity. Addition of trehalose to the films increases the stability further, especially for films maintained at low humidity. These stable hybrid film structures are promising for further studies towards developing new phototransformation devices for biotechnological applications.

1. Introduction

Photosynthetic reaction centers (RCs) are naturally occurring nano-sized structures, with dimensions on the order of 10 nm [1–3]. Porphyrins—(bacterio)chlorophylls, (B)Chls, and (bacterio)pheophytins, (B)Pheo—are the major co-factors participating in the transformation of solar light energy into an electrochemical potential (i.e., charge separation) in these naturally membrane-embedded pigment–protein supercomplexes. Other co-factors include carotenoids, quinones and cytochromes. Solar energy-conversion proceeds with an efficiency of almost 100%. Theoretical calculations indicate that the photoconversion efficiency of hybrid assemblies on the basis of native photosynthetic RCs may potentially increase the efficiency of silicon batteries by 17%–20% [4,5]. However, for the successful assembly of efficient hybrid energy-converting devices based on photosynthetic RCs, several problems remain to be solved.

First, photoprotection and repair mechanisms are absent—or at least, much less efficient—*in vitro*. Thus, stability of isolated RCs has to be considerably improved. Second, the efficiency of light harvesting in the region of the solar spectrum can possibly be substantially increased by filling the absorption gap of the RC spectra between the near-ultraviolet/blue and the near-infrared absorption regions of BChls (350–740 nm). Moreover, monolayers of isolated RCs have very low optical densities. Therefore, approaches using hybrid assemblies, i.e. consisting of plasmonic materials and/or semiconductor nanocrystals and RCs appear to be promising [6,7].

Quantum dots (QDs)—fluorescent semiconductor nanocrystals—have unique optical properties, which render them attractive for a wide range

* Corresponding author.
E-mail address: vz.paschenko@gmail.com (V.Z. Paschenko).

http://dx.doi.org/10.1016/j.jphotobiol.2016.09.009
1011-1344/

of applications in biology and medicine, as reviewed, e.g. in Oleynikov et al. [8]. The most important properties are

i) large absorption cross-sections (their extinction coefficients are several ten times higher than those of organic dyes)
ii) extremely high photostability
iii) broad absorption spectra
iv) narrow fluorescence spectra
v) the fluorescence quantum yield of QDs is, moreover, on the order of 70% [8,9].

Notably, the emission maximum of QDs depends on their diameter. For cadmium selenide (CdSe/ZnS) nanocrystals with core diameters of 2.5 to 6 nm, which are covered by zinc sulphide the fluorescence spectrum can be tuned in the range between 480 and 600 nm [8,10]. For cadmium telluride (CdTe) optical tunability from 600 to 1000 nm can be achieved. Covering QDs with an additional shell of bi- or tri-functional polymers can render them water-soluble. Moreover, these functional groups increase the QDs interaction with biomolecules [11,12].

Recent studies show that QDs may be used as light-harvesting antennae for native RCs with a very high (up to 90%) efficiency of excitation energy transfer by a Förster-type resonance mechanism. Fluorescence of the acceptors (RCs and other photosynthetic pigment–protein complexes) can be enhanced by a factor of 4 to 5, potentially even up to 300 [6,13,14]. Therefore, QDs (and other nano-structured materials) can be used to increase the light-conversion efficiency of hybrid devices based on RCs.

One promising approach to increase the stability (over time, at elevated temperatures, etc.) of such hybrid systems may be their inclusion into liposomes. Liposomes are thought to mimic the native environment of membrane proteins (such as RCs) due to interaction with membrane lipids. The lipid bilayer will protect membrane proteins from denaturation and provides the required environment for effective functions and mutual interactions of proteins. Lipids are known to influence the activity of membrane-bound enzymes [15,16]. This also holds for membrane-bound photosynthetic pigment–protein complexes, such as light-harvesting antenna complexes and RCs. However, the sensitivity of structure and function of transmembrane helices to lipid properties such as the lateral packaging, the width of the hydrophobic region as well as to the charge of the head groups should be taken into account. Moreover, also the association of transmembrane protein segments and their tilt with respect to the surface normal of the bilayer may be altered [17].

Phosphatidylcholin is the main lipid component of bacterial photosynthetic membranes, even through their lipid composition can vary considerably depending on the growth conditions, in particular, oxygen contents [18–20]. Following even intensive purification, some lipids, in particular, cardiolipin, phosphatidylcholin and glucosylgalactosyldiacylglycerol still remain closely associated with the protein subunits of the RCs of *Rhodobacter (Rb.) sphaeroides* [21]. This suggests specific interactions of these phospholipids with the RCs. Moreover, the thermodynamics and kinetics of electron transport via the quinone acceptor of the purple bacterial RCs depends of the presence of physiologically important lipids in its vicinity—phosphatidylcholin, phosphatidylglycerol, phosphatidylethanolamin and cardiolipin [22,23]. The mechanism by which lipids influence the photosynthetic energy conversion processes is not understood in detail. Probably, electrostatic effects of anionic phospholipids influence the long-lived charge-separated state at the level of the primary quinone acceptor, as previously suggested by Agostiano et al. (2005). Our work also indicates that the electron transport processes within the RCs, in particular, those involving the quinone acceptor, are substantially influenced by the dynamic state of the RC. Intermolecular mobility of different regions of RCs (which can be considered as molecular probes) is correlated to the kinetics of electron transport within a particular component of the photosynthetic electron transport chain. Such conformational changes are revealed by the temperature and the hydration state dependencies [24–26].

An alternative approach to achieve functional stability of hybrid light-converting systems *in vitro* is to use slightly dehydrated samples (thin films) which can be generated, in particular, by the addition of substances such as trehalose to stabilize the protein structures. Such substances are known to confer high stability against denaturation and help to retain functional activity of the proteins, at least to some extent [27].

In the current study, photosynthetic RCs from the purple bacterium *Rb. sphaeroides* and QDs were incorporated into liposomes based on phosphatidylcholin (lecithin). The functional properties of these hybrid complexes were investigated with regard to their potential applications in biotechnology. Conditions to achieve long-term functional stability of hybrid RC–QD complexes in thin film samples are also reported in the following.

2. Materials and methods

2.1. Preparation of reaction centers

Cells of wild type non-sulfur purple bacteria *Rb. sphaeroides*, were grown under anaerobic conditions in a luminostat at a temperature of 30 °C for 5–6 days. Cells were disrupted with an ultrasonic disintegrator. Chromatophores were collected by centrifugation and incubated for 30 min at 4 °C in 10 mM sodium phosphate buffer, pH 7.0, containing 0.5% lauryldimethyl ammonium oxid (LDAO). Following the centrifugation for 90 min at 144,000 *g* and 4 °C the supernatant containing the RCs was subjected to hydroxyl-apatite column chromatography as described in detail by Zakharova and Churbanova [28]. RCs were resuspended to a concentration of 10 μM in 10 mM sodium phosphate buffer, pH 7.0, containing 0.05% LDAO. The photoreactivity of the sample was assayed by light-induced absorption changes in the Q_y absorption band of photoactive BChl at 870 nm (P870).

2.2. Quantum dots

In the current study, CdSe/ZnS QDs with a hydrophilic polymer coating with carboxyl groups (Rusnanotech-Dubna, Russia) and emission maximum photoluminescence at 530 nm and 580 nm were used.

2.3. Preparations of liposomes

To prepare liposomes with L-α-lecithin from soybean (Sigma, USA) two different methods were used. The first was a comparatively new method of preparing single-walled vesicles by repeated pressing (extrusion) of a multilayer lipid vesicle suspension through a porous polycarbonate membrane (in our case, the pore size was 0.1 μm) in a special device—Extruder (Avanti Polar Lipids, Inc., USA). In another method, both a detergent and dialysis were used (D–D).

The method of preparing vesicles using detergent and dialysis (D–D) included the following steps:

1. 50 mg lecithin was dissolved in 0.5 ml of chloroform and evaporated
2. the lipid film was covered with 2 ml of 50 mM Tris–HCl buffer (pH 8) containing 2% sodium cholate
3. the lipid suspension was sonicated with an ultrasonic disintegrator until it became clear
4. a 0.5-ml aliquot of the resulting lipid solution in Tris buffer was supplemented with 0.2 ml of Tris buffer, sonicated for 5 s, and used for preparing lecithin liposomes
5. a 0.5-ml aliquot of the resulting lipid solution in Tris buffer was supplemented with 0.1 ml of Tris buffer and 0.1 ml of RCs (42 μM), sonicated for 5 s, and used for preparing RC-containing proteoliposomes

6. a 0.5-ml aliquot of the resulting lipid solution in Tris buffer was supplemented with 0.1 ml of Tris buffer and 0.1 ml of quantum dots (43 μM), sonicated for 5 s, and used for preparing QD-containing liposomes
7. a 0.5-ml aliquot of the resulting lipid solution in Tris buffer was supplemented with 0.1 ml of RCs (42 μM) and 0.1 ml of quantum dots (43 μM), sonicated for 5 s, and used for preparing RC/QD-containing proteoliposomes
8. the samples (4–7) were placed into dialysis bags and on a stirrer placed into a refrigerator to dialyze against 1 l of 50 mM Tris buffer (pH 8).

Using the extruder, 50 mg lecithin was also dissolved in 0.5 ml of chloroform (analytical grade) and the solvent was slowly evaporated. Then, 2 ml of 50 mM Tris buffer (pH 8) was added and the lipid was dissolved in the buffer using a vortex mixer. To accelerate dissolution, the suspension was frozen and thawed repeatedly. Solutions containing lipids and QDs, lipids and RCs, as well as lipids and mixtures of QDs with RCs were prepared in the same ratios as described above for the D–D method, but instead of the ultrasonic treatment the solutions were mixed with a vortex mixer. Later, the lipid solution or lipids containing QDs, RCs and RCs/QDs were pressed thirteen times through a membrane with 0.1 μm pores using the extruder.

2.4. Light scattering measurements

The mean size of the resulting liposomes was measured with a Z-sizer (Malvern, USA) that allowed us to determine the hydrodynamic radius of the particle by changes in their light scattering. Each measurement was repeated five times, and the results were averaged.

2.5. Transmission electron microscopy

Samples for transmission cryoelectron microscopy were prepared in the Shubnikov Institute of Crystallography, Russian Academy of Sciences, using a Vitrobot Mark IV device (FEI, Netherlands) that automatically controls the humidity and temperature. Technical details of the device and method are described in [29,30]. A support (Quantifoil, Germany) pretreated for 45 s in a smoldering charge atmosphere was placed into a chamber with controlled temperature and ultrasound emitter to create the humidity (up to 100% relative humidity). On the support, 3 μl of the sample suspension was placed. The excess fluid was automatically removed with paper filters. Thin films produced in the support holes were instantly frozen by quick submerging of the sample into liquid ethane. In our experiments, the samples were pretreated at 37 °C and 100% relative humidity.

The supports with the samples were examined with a CM-12 transmission electron microscope (Philips, Netherlands). During the experiment the voltage was 120 kV and the pressure $<0.2\cdot10^{-3}$ Pa. Microphotographs were obtained using the technology of imaging plates under standard conditions of exposure in the regime of "low dose" of electrons per Å^2.

2.6. Electrophoresis

For electrophoresis, 10-μl aliquots of freshly prepared aqueous samples (for the doubling experiment a twofold greater volume was taken) were placed into 1% agarose gel prepared in 0.25-fold TBE buffer (54 g Tris, 27.5 g boric acid, 20 ml of 0.5 M EDTA, pH 8.0) and then placed into an electrophoretic cell with 0.5-fold TBA buffer. The gel was kept for 60 min at a voltage of 80 V using a BioRad electrophoretic system (USA) and then photographed under ultraviolet illumination on a GeneGenius system (USA).

2.7. Film preparations

For the preparation of trehalose containing films the initial concentration of trehalose in the suspension was 0.144 g/ml [31]. Film samples were stored under several conditions: at room temperature (RT), i.e., 22 °C and a humidity of ~60%, at a decreased temperature of 6 °C and a humidity of ~60%, as well as at RT and a decreased humidity of ~12%. The humidity of the samples was maintained by placing them in a closed environment with saturated salt solution [32].

2.8. Absorbance and fluorescence spectroscopy

The changes in the RC absorbance were measured at 600 nm (Q_x band of P870) or 870 nm (Q_y band) using a laboratory flash-photolysis setup with the probing beam passing a double monochromator before and after of the sample and excitation by Nd-YAG laser LS-2131 M (532 nm, 8 ns, 15 mJ, Lotis-TII, Belarus).

The fluorescence excitation spectra of the samples were recorded using a SPEX Fluorolog II spectrofluorimeter (Jobin Yvon, France). Fluorescence kinetics were measured using a pulse fluorimeter excited with picosecond light pulses ($\lambda_{ex} = 532$ nm, FWHM ~20 ps) at a frequency of 1 Hz from a PIKAR-1 laser (Moscow State University, Russia). A sample of 0.5 ml was placed into a cuvette of 2 mm thickness, the optical density at $\lambda = 532$ nm being 0.1. The fluorescence kinetics were recorded using an AGAT SFZ electro-optical chamber (Russia) connected with a computer through a C7041 multichannel matrix detector and a C7557 controller (HAMAMATSU, Japan). The time resolution of the system was ~2 ps. During the experiment, the samples were stirred with a magnetic stirrer. To improve the signal/noise ratios, 50 kinetic traces were accumulated and averaged. The accumulated experimental kinetics were approximated bi-exponentially by modeling the curve as $I(t) = A_1\exp(-t/\tau_1) + A_2\exp(-t/\tau_2)$ convoluted with the apparatus characteristic function of the fluorimeter, where $I(t)$ is the fluorescence change of the sample with time; and τ_1, τ_2 and A_1, A_2 are lifetimes and amplitudes of the fast (1) and slow (2) components of the fluorescence decay kinetics. A characteristic average decay time (τ_{avr}) can be defined as follows: $\tau_{avr} = (A_1\cdot\tau_1 + A_2\cdot\tau_2)/(A_1 + A_2)$, where $A_1 + A_2 = 100$.

Fluorescence lifetimes of QDs in film samples have been measured in a spectrofluorometer Fluorolog-3 (Horiba Jobin Yvon Inc., France) equipped with a kinetic module TCSPC. Samples were excited with a photodiode, NanoLED, at 390 nm. Fluorescence kinetics were analyzed by the Fluorescence Decay Analysis Software (DAS-6), which is included into the software of the fluorometer. Decay kinetics are best approximated by the sum of three exponential functions. The mean lifetime is calculated according to the equation: $\tau_{avr} = (A_1\cdot\tau_1 + A_2\cdot\tau_2 + A_3\cdot\tau_3)/(A_1 + A_2 + A_3)$ with τ_i and A_i being the characteristic lifetimes and amplitudes of each component, respectively, with $A_1 + A_2 + A_3 = 100$.

3. Results and discussion

3.1. Comparison of liposomes produced by extrusion or detergent and dialysis

(a) *Size distribution:*

Noteworthy, the size of the vesicles depends on the protein/lipid ratio. The liposomes become smaller with higher protein content [33]. For the dioleylphosphatidylcholin to RC ratios of 8.000:1, 2.000:1, 1.000:1 used in this study the hydrodynamic radii were 21 ± 2, 35 ± 3 and 55 ± 6 nm, respectively. The average radius of proteoliposomes containing RCs in our study was ~46 ± 4 nm, the average radius of proteoliposomes containing RCs and QDs was ~44 ± 4 nm, liposomes containing only QDs had a radius of ~27 ± 3 nm (Fig. 1).

Orientation of the RCs from *Rb. sphaeroides* in liposomes (prepared by the DD method) has been assessed by their functional interaction with exogenously added cytochrome *c*, their natural

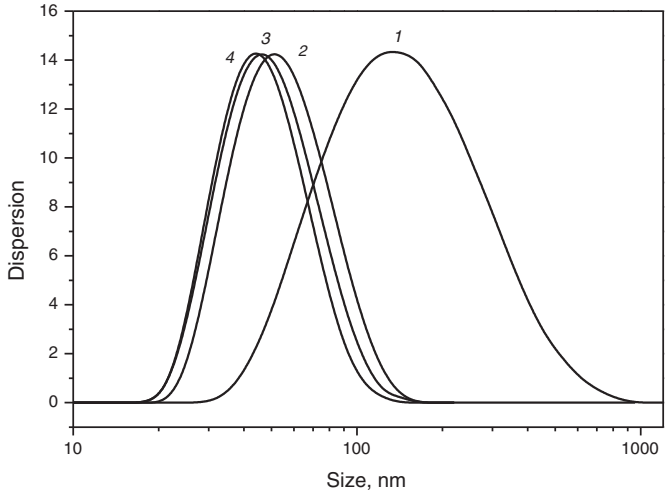

Fig. 1. Size distribution of liposomes produced by (1) extrusion through a porous polycarbonate membrane and (2) by detergent and dialysis treatment; and of proteoliposomes produced by the detergent and dialysis method containing (3) RCs and (4) RCs + QDs.

electron donor [34]. The transmembrane orientation of the RCs was such that between 45% and 85% of the donor (BChl P) was exposed to the outside, somewhat depending on the size of the liposomes.

(b) *Electron microscopy:*
A characteristic feature of liposomes produced by the extrusion approach is their double-layer structure, with an average diameter of the outer and inner layers being 120 and 60 nm, respectively, visible in the electron microscopy (Fig. 2). Liposomes produced by the DD method reveal a spherical morphology with an average diameter of about 30 nm. Moreover, larger elliptical structures about 25–30 nm wide and 120–250 nm long are found as well. The latter are probably caused by a coagulation processes of smaller particles. Dense particles became visible in the electron microscopic images upon addition of QDs. We assume that these dense particles correspond to the QDs, based on following considerations:
First, the size of those particles is about 5 nm, which corresponds to the theoretically expected dimensions of the QD-core. A similar size for such QDs has been observed previously (Shan et al. 2005). Second, the dark color indicates a rather high density, again in agreement with a CdSe-core of the QDs. Third, the dense particles are in direct contact with liposomes that indicate the association of liposomes with QDs in correspondence with the results of agarose gel electrophoresis (see below). Notably, the polymer-COOH covered QDs are interacting with the lipid bilayer of phosphatidylcholin liposomes by an unknown mechanism rather than being simply encapsulated, as was proposed previously [35].

(c) *Agarose gel electrophoresis:*
Interaction of QDs with liposomes was studied by agarose gel electrophoresis. QDs possess no mobility in the electrical field: the fluorescence signal in the agarose gel obtained by illumination of QDs with UV light remains localized at their starting position (Fig. 3). The liposomes with QDs, however, reveal a somewhat blurred fluorescent feature, which can most probably be explained by the size distribution of the liposomes (see Figs. 1 and 3). The decrease of the fluorescence signal may be an indication for a partial fluorescence quenching by the phospholipids [35,36]. An addition of the RCs to liposomes with QDs had practically no influence on their mobility in the agarose gel (data not shown).

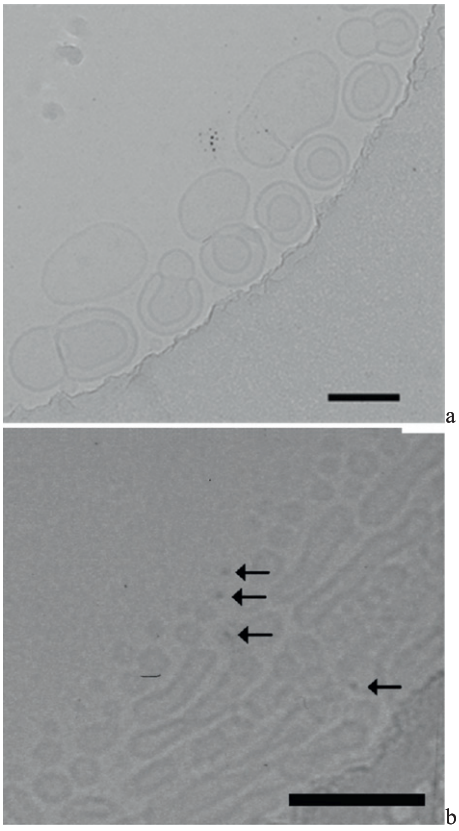

Fig. 2. Transmission electron microphotograph of liposomes prepared by the extrusion method (a) and by the D–D method (b). The marker corresponds to 120 nm. Arrows designate QDs.

3.2. Functional properties of hybrid RC–QD complexes embedded into liposomes

The absorption spectrum of RCs seems to be unaltered by the integration into liposomes (see Fig. 9). For vesicles containing QDs, a characteristic absorption with features in the region between 400 and 550 nm (similar to QDs absorption) is visible (Fig. 4). This indicates that the structural integrity of RCs is neither influenced by the high detergent (sodium cholate) concentration nor by the ultrasonic treatment.

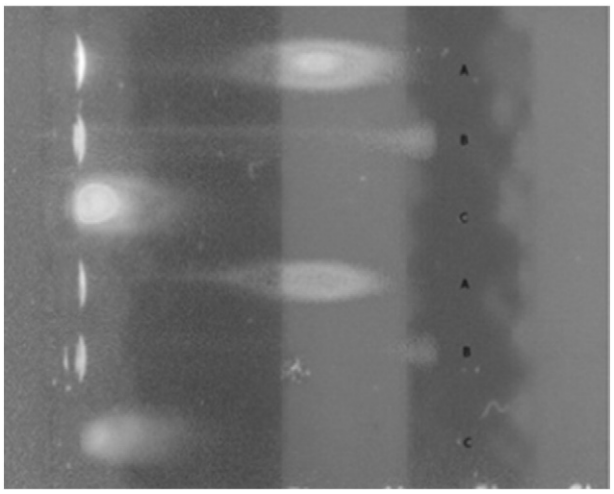

Fig. 3. Agarose gel electrophoresis image (UV illuminated). (A) Liposomes with QDs produced by detergent and dialysis treatment and (B) extrusion. (C) QDs only.

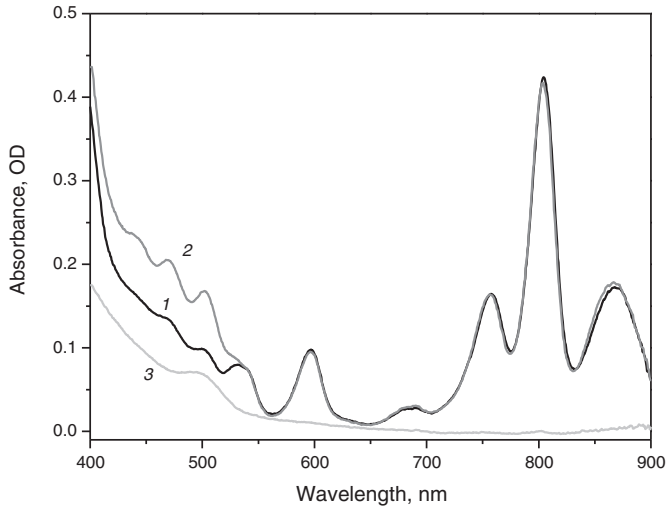

Fig. 4. Absorption spectra of lecithin proteoliposomes (1) with RCs from *Rb. sphaeroides*, (2) with RC and QDs and (3) with QDs only.

Functional activity of RCs, namely, the ability for reversible photooxidation of BChl P has been further assayed by pulsed proteoliposome excitation (Fig. 5). Kinetics of photoinduced absorption changes are related to the charge separation between the primary electron donor P870 and the quinone acceptors (Q_A, Q_B) followed by their dark recombination. RCs embedded into vesicles show very similar but not equal kinetics of dark recombination between P^+ and Q_B^- as RCs in buffer solution (curves 1 and 3). The dark recombination in proteoliposomes containing RCs and QDs, however, proceeds faster as compared to vesicles without QDs (curve 2). This is probably due to the changes in the efficiency of the temporal stabilization of the reduced quinone-acceptor Q_A of the RC. The effective electrostatic stabilization of the photoactivated electron in the quinone acceptors Q_A and Q_B of the RC of purple bacteria is achieved by a proton transfer in the protein environment. In such processes, protonated amino acid residues located in a distance up to 15–17 Å from the quinone co-factor can be involved [37–39]. It has been shown that the rate constant of the dark back-transport of the electron from the Q_B^- to P^+ is sensible to the ionization state

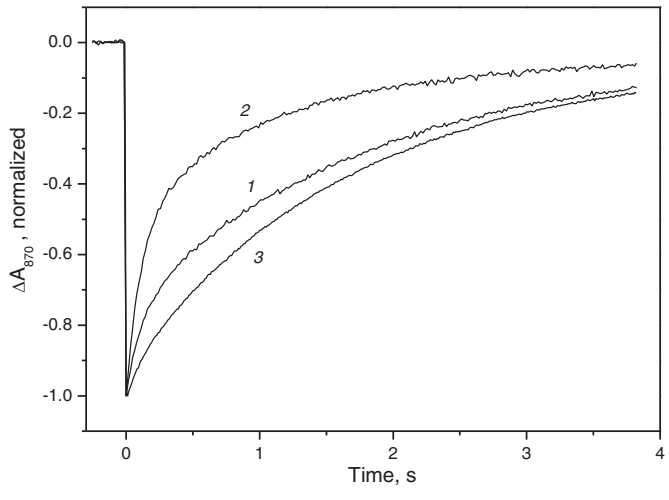

Fig. 5. Transient absorption changes of bacteriochlorophyll P870 upon excitation with a Nd-YAG laser at 532 nm in proteoliposomes with RCs (1), RCs + QDs in a ratio of 1:1 (2) and RCs in buffer solution (3).The decays for curves 1 and 2 were approximated by the sum of two exponentials with the parameters $\tau_1 = 0.128 \pm 0.004$ s ($A_1 = 0.26 \pm 0.004$) and $\tau_2 = 1.826 \pm 0.016$ s ($A_2 = 0.734 \pm 0.001$); $\tau_1 = 0.118 \pm 0.002$ s ($A_1 = 0.5340 \pm 0.004$) and $\tau_2 = 1.1550 \pm 0.015$ s ($A_2 = 0.454 \pm 0.003$), correspondingly. The decay for curve 3 was approximated by one exponential with $\tau = 1.682 \pm 0.004$ s.

of all charged residues in the vicinity of Q_B (Paddock et al. 1994). The apparent influence of the QDs on the temporal stabilization is probably indicative for their close distance to the RC within the liposome and, thereby, their influence on the structural dynamics in the peripheral regions of the RCs as well.

Effective interaction of RCs and QDs within liposomes is also confirmed by the analysis of the fluorescence properties of these hybrid complexes. Fig. 6 shows fluorescence excitation spectra of the RCs embedded into the proteoliposomes (curve 1) and upon the addition of QDs (curve 2) at different detection wavelength, respectively, (a) 775 nm, (b) 860 nm and (c) 910 nm. Without QDs the fluorescence excitation spectrum essentially reproduces the absorption spectrum of the RCs with some changes most pronounced in the Soret band (at around 400 nm). The total fluorescence yield increases substantially upon addition of QDs (Fig. 6). This can be explained by light absorption of QDs between 250 and 550 nm followed by the effective excitation energy transfer to the RCs.

Note that the fluorescence maximum of the QDs used in this study is around 530 nm, i.e. close to the Q_x band (~540 nm) of the BPheo in the RC. Moreover, the highest increase of the total fluorescence yield from

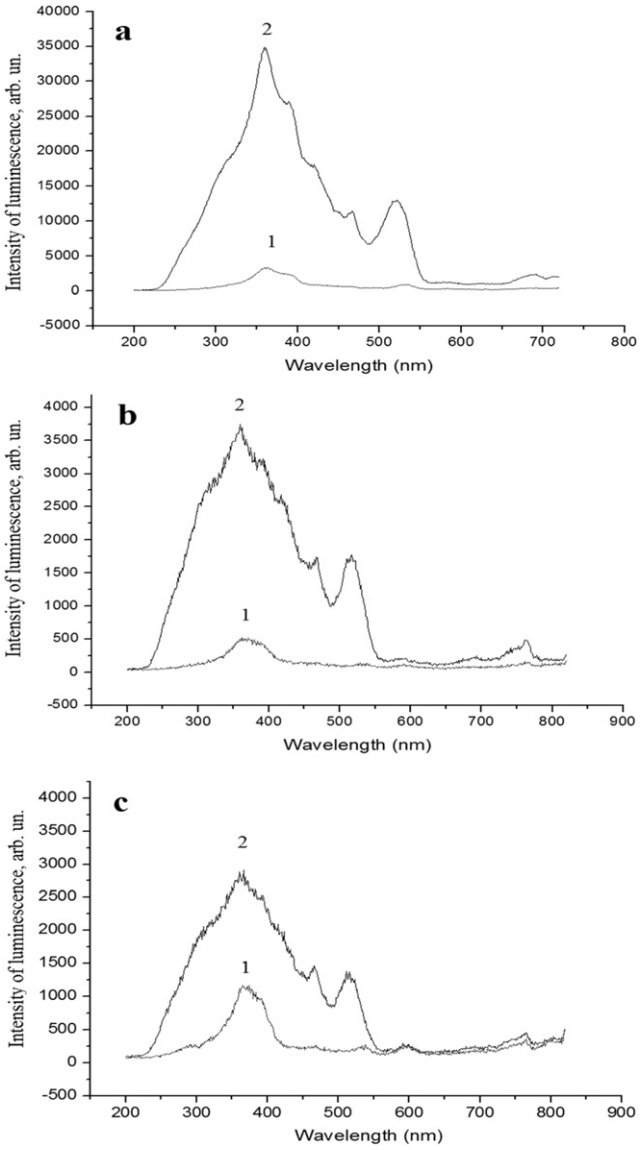

Fig. 6. Fluorescence excitation spectra of proteoliposomes containing RCs (1) and RCs + QDs in a ratio 1:1 (2) detected at different wavelengths, 775 nm (a), 860 nm (b) and 910 nm (c).

hybrid complexes is observed at a detection wavelength of the 775 nm, i.e. close to the fluorescence maximum of the BPheo (with its Q_y absorption band located at around 760 nm). The energy absorbed by the BPheo will be initially transferred to the monomeric BChl (with a Q_y absorption band at around 800 nm) and then further to the photoactive BChl P (with a Q_y maximum at around 870 nm). Correspondingly, fluorescence excitation spectra detected at 860 nm and 910 nm reveal a somewhat lowered effective increase of the fluorescence yield of the RC as caused by the interaction of the RC with QDs.

The effective decay of excited states of QDs embedded in liposomes due to their interaction with RCs in surrounding solution is also revealed in the time-resolved fluorescence signals from the QDs. The temporal profile of the fluorescence decay kinetics can be approximated by the sum of two exponential functions. RCs have been added with increasing concentration from 1 to 11 mM to the liposome samples containing QDs obtained by dialysis. Table 1 summarizes the results of the fitting analysis.

Analysis of the data reveals that fluorescence of QDs decays faster with increasing concentration of RCs. This can be explained by a "dynamic quenching" character of the decay process. This finding is also corroborated by the dependence of the fluorescence signal on RC concentration when plotted in Stern–Volmer coordinates, i.e. the ratio of maximal fluorescence (F_0, in the absence of a quencher) to actual fluorescence (F, in the presence of a quencher) vs. quencher concentration. Fig. 7 shows a linear dependence of this ratio vs. increasing RC concentration, in correspondence with dynamical quenching character of the decay processes [40].

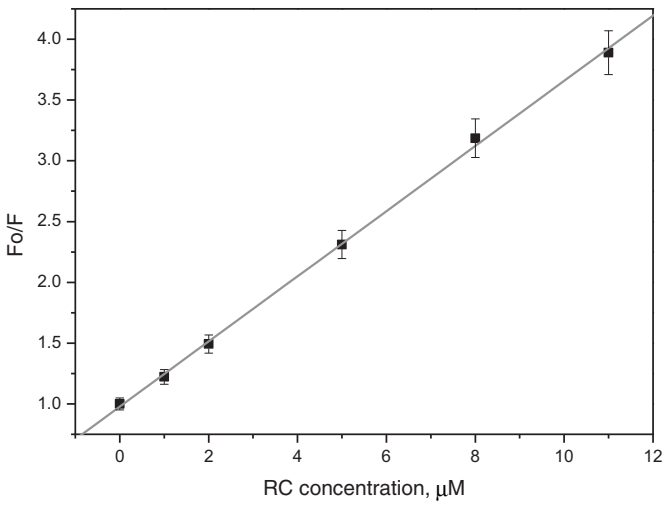

Fig. 7. Dependence of fluorescence quenching in proteoliposomes containing QDs (concentration ~1 μM) as a function of RC concentration (Stern–Volmer plot).

3.3. Functional stability of liposome-embedded samples

To estimate the functional stability of RCs embedded into liposomes the characteristic dark recombination time (τ) of P^+ and Q_A^- has been studied as a function of temperature. This functional parameter may be taken as indicative for the structural–dynamical state of the RCs and its activity. In isolated RCs the characteristic reaction time decreases substantially with rising temperature above room temperature as shown previously [41]. All observed effects remained essentially reversible up to ~50 °C. This confirms the loss of the efficiency in the temporal stabilization of the charge-separated state P^+ and Q_A^-. The observed effects can be understood in terms of the dynamics of hydrogen bonds in the vicinity of the co-factors responsible for electron transfer to the RC [42,43].

To study the temperature dependence of P^+ and Q_A^- recombination in RCs embedded into liposomes o-phenanthroline (up to 10^{-2} M) has been added to the samples. This inhibits the direct light-induced transfer of electrons from the primary quinone acceptor to the secondary one. Samples were excited by single light flashes. Initially, at room temperature, the recombination time in RCs embedded into liposomes and RCs in buffer solution is very similar with characteristic time constants τ of 100 ms and 95 ms, respectively. Substantial differences with respect to the control (RCs in buffer solution) have been observed, however, upon heating of the samples. Namely, while at temperatures exceeding room temperature, the recombination time decreases for RCs in buffer solution, a slight increase in the recombination time has been observed for RCs embedded into liposomes even at 50 °C (see Fig. 8). This indicates that in a liposomal environment, the stabilization efficiency of the photo-separated charges P^+ and Q_A^- remains largely unaltered, even at 50 °C.

Thus, the temperature dependence of the electron transfer rate in RCs is substantially influenced by some unknown interaction mechanism between RCs and the artificial lipid membrane. The latter is also corroborated by the direct comparison of absorption spectra obtained at 20 °C and 50 °C for both samples.

Absorption spectra of RCs from *Rb. sphaeroides* obtained at 20 °C (solid line) and 50 °C (dashed line) for RCs in liposomes are shown in Fig. 9(a). Note that (in the near-infrared spectral region) the relation between the absorption bands corresponding to BPheo (at 760 nm), the monomeric BChl (at 800 nm) and the photoactive BChl (at 860 nm) remains almost unaltered upon increasing the temperature. For RCs in buffer solution, however, pheophytinisation, i.e. the loss of the central Mg^{++} ion from the BChl molecules becomes visible (Fig. 9(b), dashed line). Namely, the magnitudes of the 800 nm and 860 nm absorption bands which correspond to the BChl monomer and dimer, respectively, decrease while the magnitude of the BPheo absorption band at 760 nm increases.

3.4. Functional activity and stability of thin film samples

By drying a drop of the RC suspension on the glass substrate, a certain amount of pheophytinisation is observed as shown in Fig. 10 (black solid line 2). Note the amplitude ratio in the absorption spectrum for wavelengths of 760, 800 and 860 nm was 0.57:1:0.41, respectively. The amount of pheophytinisation increases slightly upon storage of the samples for 5 months (147 days in total) at RT and a relative humidity of ~60% (Fig. 10 grey solid line 2). A decrease

Table 1
Amplitudes (A) and characteristic lifetimes (τ) of fluorescence decay kinetics of QDs embedded in liposomes, depending on the concentration of added RCs.

Sample	Amplitude A_1 (%)	Lifetime τ_1, ps	Amplitude A_2 (%)	Lifetime τ_2, ps	Average lifetime τ_{avr}, ps
QD, 1 μM	38 ± 2	205 ± 10	62 ± 3	4047 ± 200	2590 ± 150
QD + 1 μM RC	45 ± 2	241 ± 10	55 ± 3	3785 ± 200	2174 ± 150
QD + 2 μM RC	50 ± 3	220 ± 10	50 ± 3	3274 ± 200	1747 ± 120
QD + 5 μM RC	56 ± 3	214 ± 10	44 ± 2	2337 ± 150	1139 ± 120
QD + 8 μM RC	62 ± 3	208 ± 10	38 ± 2	1832 ± 150	826 ± 100
QD + 11 μM RC	64 ± 3	183 ± 10	36 ± 2	1540 ± 150	674 ± 80

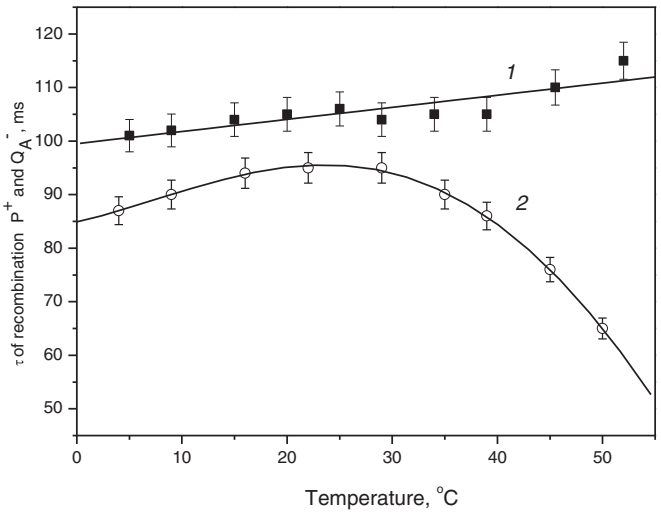

Fig. 8. Temperature dependence of the characteristic time constants for dark recombination of the charge-separation between P^+ and Q_A^- in RCs of *Rb. sphaeroides* embedded into lecithin liposomes (1, closed squares) or RCs in buffer solution (2, open circles). Electron transfer from Q_A^- to Q_B was blocked by o-phenanthroline.

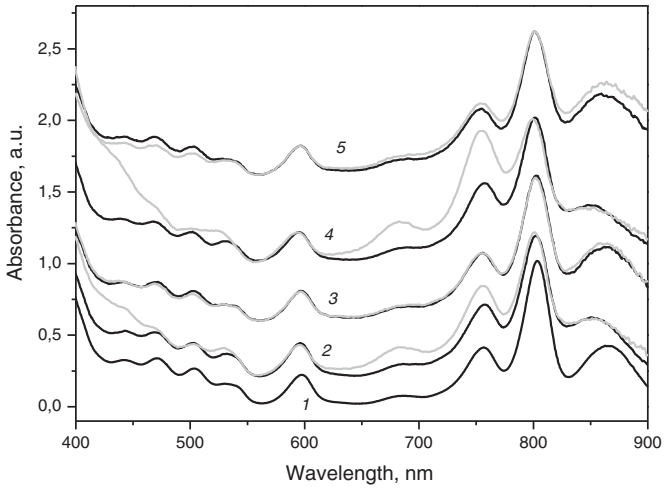

Fig. 10. Absorption spectra of a RC–water suspension (line 1), air-dried RC films prepared without trehalose (lines 2 and 4), air-dried RC films prepared with trehalose (lines 3 and 5), 24 h after preparation (black lines). Grey lines show the absorption of samples after 5 months of storage under different conditions: RT and 60% humidity (lines 2 and 3), RT and 12% relative humidity (lines 4 and 5). All spectra were normalized at the 800 nm absorption band.

of the storage temperature of RC films to 6 °C slowed down the pheophytinisation process (data not shown). For films stored at RT and a relative humidity of 12%, a substantial pheophytinisation was observed (Fig. 10, line 4). The ratio of the absorption maxima at 760, 800 and 860 nm was 0.54:1:0.39 following 14 days of storage and, correspondingly, changed to 0.91:1:0.37 following 5 months of storage (Fig. 10, grey line 4).

A reduced stability of RC film samples stored at 12% relative humidity is most probably explained by a substantial increase of the detergent concentration, which is used to solubilize the RC. As we have shown recently, RC films from *Rb. sphaeroides*, which are stored under conditions of 90% to 40% relative humidity, retain a stable content of water of about 20% with respect to its mass. This amount of water (20% to 30%) corresponds to the water content incorporated by different proteins into an

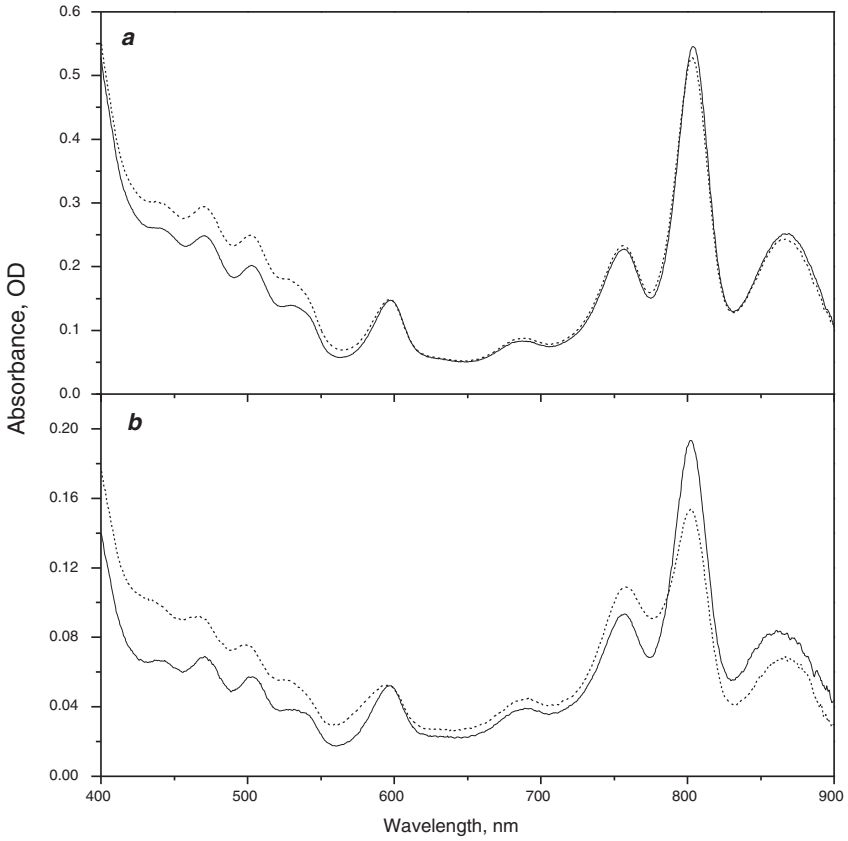

Fig. 9. Absorption spectra of RCs from *Rb. sphaeroides* in liposomes (a) and in buffer solution (b) at 20 °C (solid line) and 50 °C (dashed line).

initial hydrating shell, which covers macromolecules. Upon drying of RC samples under relative humidity in the range of 40% to 12%, the water content decreases by a factor of 2 and reaches 10% relative to protein mass at 12% relative humidity [44].

Addition of trehalose to buffer-suspended RCs prior to dry film preparation reveals a pronounced protective effect. In particular, no pheophytinisation was observed after up to 4 months of storage at RT and a humidity 60% (Fig. 10, grey line 3). Some increase of the amplitude of 860 nm absorption band is probably related to the increase of light scattering in the sample. Importantly, the addition of trehalose has preserved the sample from pheophytinisation even after up to 147 days of storage at RT and low humidity 12%, i.e., at storage conditions at which otherwise prepared RC films (without trehalose) were dramatically degraded (Fig. 10, grey line 5).

An addition of trehalose helps not only to avoid pheophytinisation of BChl thin films but also helps to preserve the functional electron-transport activity close to the native level. This is verified by the measurement of dark recovery kinetics of photo-oxidised BChl RC (P^+) following the RC activation with single light flashes (Fig. 5). In trehalose-free films, the characteristic dark recovery time of P^+ is $\tau \approx 55 \pm 2$ ms (Fig. 11, line 6). This characterizes the recombination of the electron to P^+ from the primary quinone acceptor Q_A as a subsequent direct electron transfer from the Q_{A-} to the secondary quinone Q_B is inhibited in the dry RC film [45]. The characteristic time of this reaction for RCs in buffer at room temperature is about 100 ± 5 ms. However, this value decreases upon lowering of the temperature or also upon drying. This indicates a sensitivity of the process to the intramolecular dynamics of the RC [46]. The kinetics of dark recovery is barely changed upon further 147 days of storage of these samples at room temperature and 60% humidity (Fig. 11, line 7).

In films prepared with trehalose, the kinetics of P^+ dark recovery is approximated by two exponents with characteristic times $\tau_1 = 40 \pm 2$ ms (amplitude, $A_1 = 55\%$) and $\tau_2 = 250 \pm 5$ ms (amplitude $A_2 = 45\%$) (Fig. 11, line 1). This confirms that in the part of these RC samples, the direct electron transfer from Q_A to Q_B is retained. A return of the electron from Q_B^- to P^+ corresponds to the second P^+ recovery component with a characteristic recovery time of hundreds of ms [47,48]. The $P^+ - Q_B^-$ characteristic recombination time in water suspension is about 1 s, it can decrease, however, upon dehydration. Fig. 11 (line 5) shows that the P^+ recovery in trehalose-treated films is retarded with respect to trehalose-free films even after 147 days of storage: $\tau_1 = 30 \pm 2$ ms ($A_1 = 65\%$), $\tau_2 = 140 \pm 5$ ms ($A_2 = 35\%$).

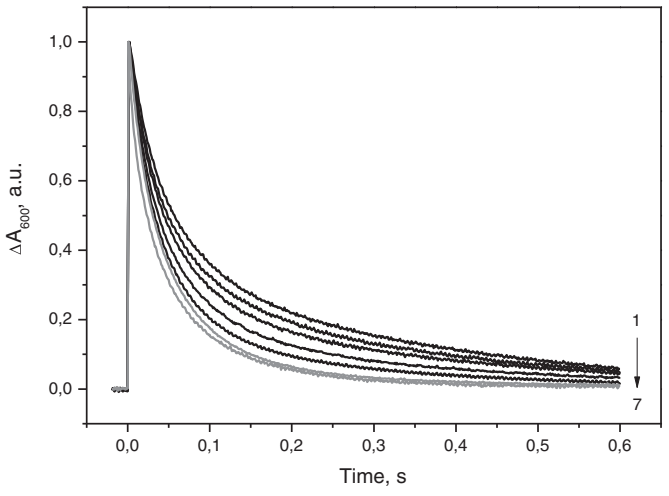

Fig. 11. Evolution of $P870^+$ dark recovery kinetics in RC films during storage at room temperature and 60% humidity. Black lines 1–5 were obtained for films with trehalose after 24 h, 8 days, 28 days, 63 days and 147 days of storage, respectively. Lines 6–7 are obtained with trehalose-free films after 24 h and 147 days of storage, respectively.

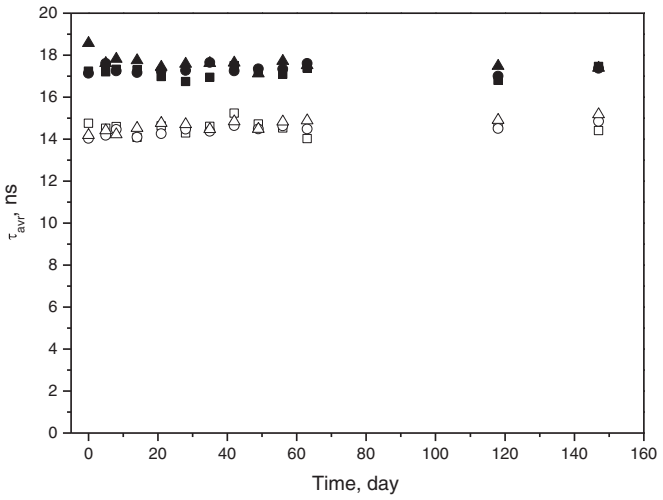

Fig. 12. Fluorescence lifetimes of QD_{580} in hybrid films at RC:QD ratios of 1:1 (closed symbols) and 5:1 (open symbols) depending on storage time. Storage conditions: RT; relative humidity of 60% (squares), 12% (circles) as well as 6 °C and 60% humidity (triangles).

We have also measured the average fluorescence lifetime of QDs (QD580) in hybrid film structures prepared at two different RC/QD ratios 1:1 and 5:1 depending on storage time under different storage conditions, namely, under room temperature and 60% humidity, under room temperature and 12% humidity and also under 6 °C temperature and 60% humidity.

Decay kinetics are best approximated by the sum of three exponential functions.

Fig. 12 shows that the fluorescence lifetime decreases with an increasing concentration of RCs (acting as quenchers). Moreover, the characteristic lifetime remains unaltered even after long storage of films under the conditions indicated.

Fluorescence lifetimes of QDs incorporated into dry films were compared to those of hybrid structures (QDs + RCs) depending on relative humidity (at 22 °C). Fig. 13 (lines 1 and 2) shows that fluorescence lifetimes of QDs in film and hybrid structures increases systematically with the decrease of sample humidity but to a higher extent in the first case. This leads to an increase in the ratio of τ_{avr} values obtained for QD containing films and hybrid QD-RC films with decreasing humidity. In

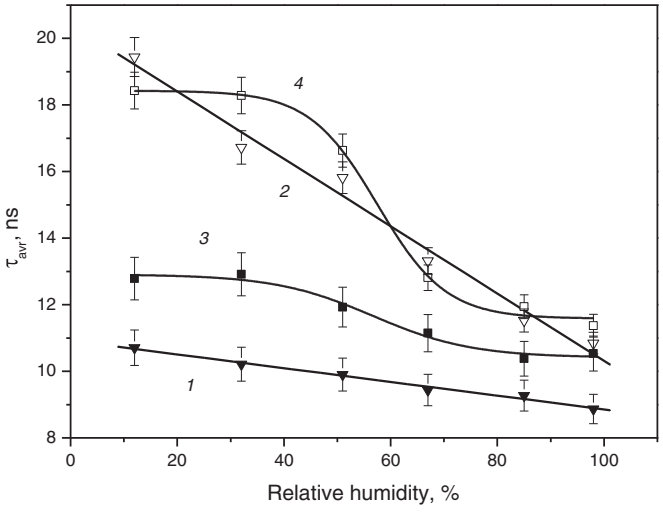

Fig. 13. Dependence of average fluorescence lifetime on humidity in dry films. QD_{580} only (lines 2 and 4) and in hybrid-film structure QD_{580}/RC with the 1:2.3 ratio (lines 1 and 3). Lines 1 and 2 correspond to trehalose-free, lines 3 and 4 trehalose-containing samples. Room temperature.

terms of the Förster theory, that means an increase of excitation energy transfer between QDs and RCs in hybrid structures. Such enhancement of energy transfer upon decrease of humidity of hybrid films is probably due to a decreasing distance between QDs and RCs upon matrix dehydration. In trehalose-treated samples, the dependence of fluorescence lifetime on humidity of the environment reveals a similar tendency but the shape is clearly sigmoidal (Fig. 13, lines 3 and 4). Obviously, this effect is related to the presence of trehalose. The mechanism by which this disaccharide interacts with the surface of macromolecules as well as the exact mechanism that is responsible for the protection of proteins from denaturation (in particular, due to drying) remains the subject of further studies.

Concerning the function of trehalose to prevent a protein from denaturation, several explanations were proposed. Trehalose may stabilize proteins during drying through substitution of (hydrating) water molecules, forming hydrogen bonds directly with the surface of the respective macromolecule [49]. According to another hypothesis, upon dehydration, the trehalose helps to retain a portion of hydrating water close to the macromolecular surface, forming a glass-like (confining) layer between the macromolecule and trehalose [50,51]. Probably, the second assumption explains the observed sigmoidal behaviour of fluorescence lifetimes, which depends on humidity. Upon dehydration (or rehydration) of films containing macromolecules (QDs or QDs + RCs) in an aqueous trehalose medium in a certain range of water content, the water–trehalose structure rearranges close to the macromolecular surface (collective-like transition).

4. Conclusions

In the present work, it has been shown that efficient hybrid constructs composed of light-transforming purple bacterial RCs and inorganic nanocrystals (QDs) embedded into artificial membranous vesicular particles can be generated. The hybrid complexes were produced by self-assembly due to electrostatic interactions. Thus, stable hybrid structures have been obtained with the RCs retaining their full functional activity and QDs effectively transferring the absorbed light energy to the RCs. A reliable functional contact was shown to exist in the QD/RC complex when embedded in a lipid bilayer structure. The liposomal structure was responsible for the high resistance of the proteins to denaturation under the influence of temperature.

Remarkably, hybrid “dry” RC/QD samples stored at atmospheric humidity and temperature remain functionally active for at least several months. This was ascertained by measurements of their spectral characteristics, fluorescence lifetimes as well as electron-transport activity. Addition of the disaccharide trehalose to these samples increases their stability, especially, if the samples were stored at reduced humidity. Efficient excitation energy transfer from QDs to RCs has been observed in a broad range of humidities; however, the efficiency increases upon dehydration.

The obtained results demonstrate the possibility to create efficient artificial light-harvesting antennas for photosynthetic RCs on the basis of QDs in films. Moreover, the remarkable stability of hybrid film-structures (in particular, upon additional stabilization with trehalose)—which retains functional activity for several months—shows exciting prospects for developing novel light-harvesting (bio-hybrid) modules.

Acknowledgements

This work was supported by the Russian Foundation for Basic Research (project nos. 15-29-01167, 14-04-01536 and 13-04-00403) and the German Ministry of Education and Research, BMBF, grant no. 031A154B (to H.L.) and GAČR grant No. P501/12/G055.

References

[1] X. Hu, T. Ritz, A. Damjanovic, F. Autenrieth, K. Schulten, The photosynthetic apparatus of purple bacteria, Q. Rev. Biophys. 35 (2002) 1–62.
[2] L.M. Yoder, A.G. Cole, R.J. Sension, Structure and function in the isolated reaction center complex of Photosystem II: energy and charge transfer dynamics and mechanism, Photosynth. Res. 72 (2002) 147–158.
[3] A. Busch, M. Hippler, The structure and function of eukaryotic photosystem I, Biochim. Biophys. Acta 1807 (2011) 864–877.
[4] W. Shockley, H.J. Queisser, Detailed balance limit of efficiency of p-n junction solar cells, J. Appl. Phys. 32 (1961) 510–519.
[5] P. Wurfel, Physics of Solar Cells, Wiley-VCH, Weinheim, 2005.
[6] N. Czechowski, H. Lokstein, D. Kowalska, K. Ashraf, R.J. Cogdell, S. Mackowski, Large plasmonic fluorescence enhancement of cyanobacterial photosystem I coupled to silver island films, Appl. Phys. Lett. 105 (2014) 043701.
[7] S. Maćkowski, N. Czechowski, K.U. Ashraf, M. Szalkowski, H. Lokstein, R.J. Cogdell, D. Kowalska, Origin of bimodal fluorescence enhancement factors of *Chlorobaculum tepidum* reaction centers on silver island films, FEBS Lett. 590 (2016) 2558–2565.
[8] V.A. Oleynikov, A.V. Sukhanova, I.R. Nabiev, Fluorescent semiconductor nanocrystals for biology and medicine, Russ. Nanotechnol. 2 (2007) 160–173.
[9] C.A. Leatherdale, W.-K. Woo, F.V. Mikulec, M.G. Bawendi, On the absorption cross section of CdSe nanocrystal quantum dots, J. Phys. Chem. B 106 (2002) 7619–7622.
[10] O.I. Micic, H.M. Cheong, H. Fu, A. Zunger, J.R. Sprague, A. Mascarenhas, A.J. Nozik, Size-dependent spectroscopy of InP quantum dots, J. Phys. Chem. B101 (1997) 4904–4912.
[11] D. Gerion, F. Pinaud, S.C. Williams, W.J. Parak, D. Zanchet, S. Weiss, A.P. Alivisatos, Synthesis and properties of biocompatible water-soluble silica-coated CdSe/ZnS semiconductor quantum dots, J. Phys. Chem. B 105 (2001) 8861–8871.
[12] T. Pons, I.L. Medintz, K.E. Sapsford, S. Higashiya, A.F. Grimes, D.S. English, H. Mattoussi, On the quenching of semiconductor quantum dot photoluminescence by proximal gold nanoparticles, Nano Lett. 7 (2007) 3157–3164.
[13] I. Nabiev, A. Rakovich, A. Sukhanova, E. Lukashev, V. Zagidullin, V. Paschenko, Yu.P. Rakovich, J.F. Donegan, A.B. Rubin, A.O. Govorov, Fluorescent quantum dots as artificial antennas for enhanced light harvesting and energy transfer to photosynthetic reaction centers, Angew. Chem. 49 (2010) 7217–7221.
[14] E.G. Maksimov, T.S. Gostev, F.I. Kuzminov, N.N. Sluchanko, I.N. Stadnichuk, V.Z. Paschenko, A.B. Rubin, Quantum dots and photosensitive protein phycoerythrin hybrid systems, Russ. Nanotechnol. 5 (2010) 107–112.
[15] H. Sandermann, Regulation of membrane enzymes by lipids, Biochim. Biophys. Acta 515 (1978) 209–237.
[16] N. Latruffe, J.M. Berrez, M.S. el Kebbaj, Lipid-protein interactions in biomembranes studied through the phospholipids specificity of D-beta-hydroxybutyrate dehydrogenase, Biochimie 68 (1986) 481–491.
[17] T.K.M. Nyholm, S. Ozdirekcan, J.A. Killian, How protein transmembrane segments sense the lipid environment, Biochemistry 46 (2007) 1457–1465.
[18] B.J.B. Wood, B.W. Nichols, A.T. James, The lipids and fatty acid metabolism of photosynthetic bacteria, Biochim. Biophys. Acta 106 (1965) 261–273.
[19] J.C. Onishi, P. Niederman, *Rhodopseudomonas sphaeroides* membranes: alterations in phospholipid composition in aerobically and phototrophically grown cells, J. Bacteriol. 149 (1982) 831–839.
[20] C. Benning, Membrane lipids in anoxygenic photosynthetic bacteria, in: P.-A. Siegenthaler, N. Murata (Eds.), Advances in Photosynthesis and Respiration, vol. 6, Springer, Netherlands 2004, pp. 83–101.
[21] A. Camara-Artigas, D. Brune, J.P. Allen, Interactions between lipids and bacterial reaction centers determined by protein crystallography, Proc. Natl. Acad. Sci. U. S. A. 99 (2002) 11055–11060.
[22] A. Agostiano, F. Milano, M. Trotta, Trapping of a long-living charge separated state of photosynthetic reaction centers in proteoliposomes of negatively charged phospholipids, Photosynth. Res. 83 (2005) 53–61.
[23] F. Milano, M. Dorogi, K. Szebenyi, L. Nagy, P. Maroti, G. Varo, L. Giotta, A. Agostiano, M. Trotta, Enthalpy/entropy driven activation of the first interquinone electron transfer in bacterial photosynthetic reaction centers embedded in vesicles of physiologically important phospholipids, Bioelectrochemistry 70 (2007) 18–22.
[24] A.I. Berg, P.P. Knox, A.A. Kononenko, E.N. Frolov, N.Ya. Uspeskaja, I.N. Khrymova, A.B. Rubin, G.I. Likhtenstein, K. Hideg, Conformational mobility and functional activity of photosynthetic reaction centers of *Rhodopseudomonas sphaeroides*, Mol. Biol. (Moscow) 13 (1979) 469–477.
[25] A.I. Kotelnikov, G.I. Likhtenstein, V.R. Fogel, V.V. Kochetkov, P.P. Knox, A.A. Kononenko, N.P. Grishanova, A.B. Rubin, Molecular dynamics and electron transfer in photosynthetic reaction centers, Mol. Biol. (Moscow) 17 (1983) 846–854.
[26] A.A. Kononenko, P.P. Knox, S.K. Chamorovskii, A.B. Rubin, G.I. Likhtenstein, Yu.F. Krupianskii, I.P. Syzdalev, V.I. Goldanskii, Electron transfer and intramolecular dynamics of photosynthetic reaction centers, Chem. Phys. (Moscow) 5 (1986) 795–804.
[27] J.H. Crowe, F.A. Hoekstra, L.M. Crowe, Anhydrobiosis, Annu. Rev. Physiol. 54 (1992) 579–599.
[28] N.I. Zakharova, I.Yu. Churbanova, Methods for isolating reaction center preparations from purple photosynthetic bacteria, Biochem. Mosc. 65 (2000) 181–193.
[29] J.R. Bellare, H.T. Davis, L.E. Scriven, Y. Talmon, Controlled environment vitrification system: an improved sample preparation technique, J. Electron Microsc. Tech. 10 (1988) 87–111.
[30] P.M. Frederik, M.C. Stuart, P.H. Bomans, W.M. Busing, K.N. Burger, A.J. Verkleij, Perspective and limitations of cryo-electron microscopy. From model systems to biological specimens, J. Microsc. 161 (1991) 253–262.

[31] G. Palazzo, A. Mallardi, A. Hochkoeppler, L. Cordone, G. Venturoli, Electron transfer kinetics in photosynthetic reaction centers embedded in trehalose glasses: trapping of conformational substrates at room temperature, Biophys. J. 82 (2002) 558–568.
[32] P. Winston, D. Bates, Saturated solutions for the control of humidity in biological research, Ecology 41 (1960) 232–237.
[33] F. Milano, F. Italiano, M. Trotta, A. Agostiano, Characterisation of RC-proteoliposomes at different RC/lipid ratios, Photosynth. Res. 100 (2009) 107–112.
[34] K. Iba, K. Takamiya, H. Arata, Y. Toh, M. Nishimura, Transmembrane orientation of reaction centers in proteoliposomes from *Rhodopseudomonas sphaeroides*, J. Biochem. 96 (1984) 1823–1830.
[35] W.T. Al-Jamal, K.T. Al-Jamal, P.H. Bomans, P.M. Frederik, K. Kostarelos, Functionalized-quantum-dot–liposome hybrids as multimodal nanoparticles for cancer, Small 4 (2008) 1406–1415.
[36] R. Generalov, S. Kavaliauskiene, S. Westrøm, W. Chen, S. Kristensen, P. Juzenas, Entrapment in phospholipid vesicles quenches photoactivity of quantum dots, Int. J. Nanomedicine 6 (2011) 1875–1888.
[37] M.Y. Okamura, G. Feher, Proton transfer in reaction centers from photosynthetic bacteria, Annu. Rev. Biochem. 61 (1992) 861–896.
[38] C.R.D. Lancaster, H. Michel, B. Honig, M.R. Gunner, Calculated coupling of electron and proton transfer in the photosynthetic reaction center of *Rhodopseudomonas viridis*, Biophys. J. 70 (1996) 2469–2492.
[39] J. Miksovska, P. Maroti, J. Tandori, M. Schiffer, D.K. Hanson, P. Sebban, Distant electrostatic interactions modulate the free energy level of Q_A^- in the photosynthetic reaction center, Biochemistry 35 (1996) 15411–15417.
[40] J.R. Lakowicz, Principles of Fluorescence Spectroscopy, 2nd ed. Plenum Press, New York, 1999.
[41] P.M. Krasilnikov, P.P. Knox, E.P. Lukashev, V.Z. Paschenko, I.Yu. Churbanova, K.V. Shaitan, A.B. Rubin, Reaction of charge recombination between photooxidized bacteriochlorophyll and reduced primary quinone in *Rb. sphaeroides* reaction centers is accelerated under temperatures above 300 K, Dokl. Biochem. Biophys. 375 (2000) 828–830.
[42] P.M. Krasilnikov, P.A. Mamonov, P.P. Knox, V.Z. Paschenko, A.B. Rubin, The influence of hydrogen bonds on electron transfer rate in photosynthetic RCs, Biochim. Biophys. Acta 1767 (2007) 541–549.
[43] P.M. Krasilnikov, P.P. Knox, A.B. Rubin, Relaxation mechanism of molecular systems containing hydrogen bonds and free energy temperature dependence of reaction of charges recombination within *Rhodobacter sphaeroides* RC, Photochem. Photobiol. Sci. 8 (2009) 181–195.
[44] P.P. Knox, A.A. Kononenko, A.B. Rubin, Functional activity in photosynthetic reaction centers from *Rhodopseudomonas sphaeroides* at fixed hydration levels of the preparations, Bioorg. Chem. (USSR) 5 (1979) 879–885.
[45] R.K. Clayton, Effects of dehydration on reaction centers from *Rps. sphaeroides*, Biochim. Biophys. Acta 504 (1978) 255–264.
[46] B.H. McMahon, J.D. Muller, C.A. Wright, G.U. Nienhaus, Electron transfer and protein dynamics in the photosynthetic reaction center, Biophys. J. 74 (1998) 2567–2587.
[47] M.Y. Okamura, M.L. Paddock, M.S. Graige, G. Feher, Proton and electron transfer in bacterial reaction centers, Biochim. Biophys. Acta 1458 (2000) 148–163.
[48] L. Ambrosone, A. Mallardi, G. Palazzo, G. Venturoli, Effect of heterogeneity in the distribution of ligands and proteins among disconnected particles: the binding of ubiquinone to the bacterial reaction center, Phys. Chem. Chem. Phys. 4 (2002) 3071–3077.
[49] J.F. Carpenter, J.H. Crowe, An infrared spectroscopic study of the interaction of carbohydrates with dried proteins, Biochemistry 28 (1989) 3916–3922.
[50] P.S. Belton, A.M. Gil, IR and Raman spectroscopic studies of the interaction of trehalose with hen egg white lisozyme, Biopolymers 34 (1994) 957–961.
[51] P. Subrata, P. Sandip, Molecular insights into the role of aqueous trehalose solution on temperature-induced protein denaturation, J. Phys. Chem. B 119 (2015) 1598–1610.